International Journal on Magnetic Particle Imaging
Vol 8, No 1, Suppl 1, Article ID 2203048, 4 Pages

Infinite Science Publishing

Proceedings Article

Immobilized nanoparticles with uniaxial anisotropy in multi-dimensional Lissajous-type excitation: An equilibrium model approach

Hannes Albers [a] · Tobias Kluth [a,b,*]

[a] Center for Industrial Mathematics, University of Bremen, Bremen, Germany
[b] Center for Optimization and Approximation, University of Hamburg, Hamburg, Germany
*Corresponding author, email: tkluth@math.uni-bremen.de

Abstract

Proper modeling of the magnetization dynamics of the involved magnetic nanoparticles (MNPs) is still one of the open challenges in magnetic particle imaging (MPI) particularly in the multi-dimensional excitation case of Lissajous-type. In this simulation study we focus on the immobilized and oriented MNP case and we investigate similarities and differences between the Fokker-Planck Néel model and an equilibrium model taking into account uniaxial anisotropy.

I. Introduction

In MPI, proper modeling of the mapping from tracer concentration to induced voltage is still one of the open key challenges particularly for multi-dimensional excitation patterns such as Lissajous-type ones. One of the most important ingredients required for a proper formulation of this mapping is the dynamic behavior of the magnetic nanoparticles' magnetic moment in an applied magnetic field in a large ensemble of nanoparticles contained in the tracer material. Typically, two well-known mechanisms, Brownian and Néel rotation, need to be taken into account. In this context, the modeling strategy strongly relies on the condition of the tracer, i.e., whether we consider the fluid case or an immobilized setting. Recently, the immobilized case has become of particular interest as, on the one side, it allows for defining a new contrast [1] and, on the other side, it requires consideration of Néel rotation only for improved modeling [2]. The approach in the latter work relies on a Néel Fokker-Planck approach (Néel FP model) to obtain a dictionary of magnetic moment simulations for various easy axis orientations when assuming uniaxial anisotropy. Furthermore, a close similarity between the equilibrium model [3] and the Néel FP model without anisotropy has already been observed in [4]. This raises the immediate question for an equilibrium model taking uniaxial anisotropy into account. In this work we address this question by formulating and comparing an equilibrium model with uniaxial anisotropy (EQA) [5] to the Néel FP model.

II. Methods and materials

In a general MPI imaging experiment the setting is as follows: Let $\Omega \subset \mathbb{R}^3$ be the field-of-view containing MNPs. A voltage induced by the MNPs' in a receive coil with sensitivity profile $p : \mathbb{R}^3 \to \mathbb{R}^3$ in m^{-1} is approximately given by

$$\tilde{v}_{\mathrm{M}}(t) = -\mu_0 \int_\Omega c(r) p(r)^{\mathsf{T}} \frac{\partial}{\partial t} \bar{m}(r,t)\, \mathrm{d}r \qquad (1)$$

10.18416/ijmpi.2022.2203048

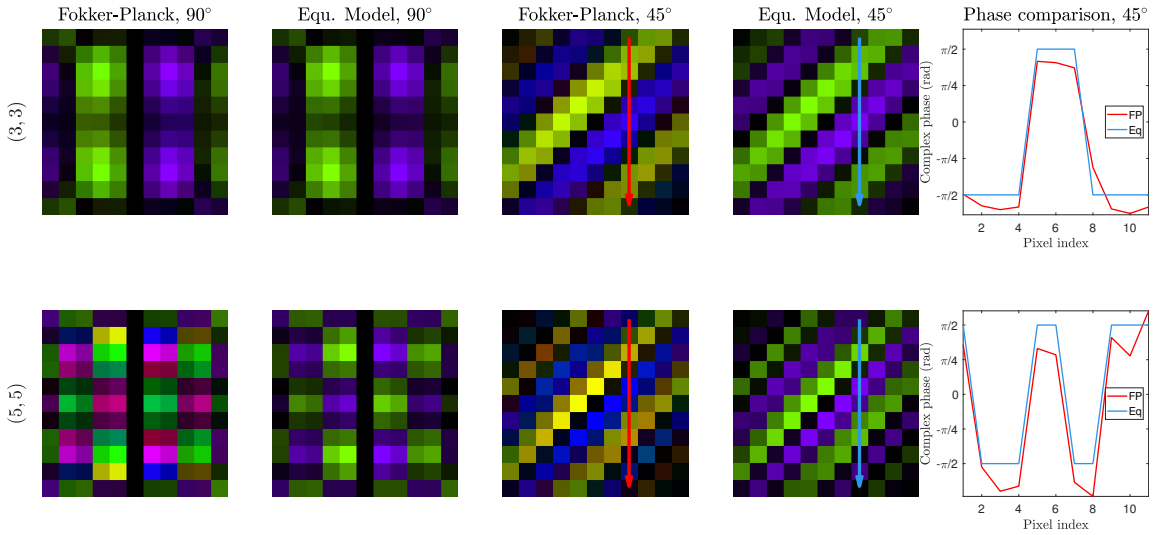

Figure 1: Two frequency components for the mixing orders $\kappa_x = \kappa_y = 3,5$ for the Néel model and the equilibrium model with anisotropy for $D = 24\,\text{nm}$, $K^{\text{anis}} = 4100\,\text{J/m}^3$. Two different easy axis orientations are shown. This visualization employs a colormap for complex numbers where the magnitude is represented by brightness and hue represents the phase [6]. For the 45° case, the complex phases along a vertical line are compared in the rightmost column.

in V where $c : \Omega \to \mathbb{R}_0^+$ in molL^{-1} is the concentration of the magnetic nanoparticles and $\bar{m} : \mathbb{R}^3 \times [0,T] \to \mathbb{R}^3$ in $10^{-3}\text{Am}^2\,\text{mol}^{-1}$ is the molar mean magnetic moment. The mean magnetic moment $\bar{m}(r,t)$ depends on the applied magnetic field $H : \mathbb{R}^3 \times [0,T] \to \mathbb{R}^3$ in $\text{T}\,\mu_0^{-1}$, which comprises a static selection field $H_{\text{SF}} : \mathbb{R}^3 \to \mathbb{R}^3$ and a dynamic drive field $H_{\text{DF}} : \mathbb{R}^3 \times [0,T] \to \mathbb{R}^3$, i.e., $H(r,t) = H_{\text{SF}}(r) + H_{\text{DF}}(r,t)$.

II.I. Néel model with uniaxial anisotropy

One important aspect in the model equation (1) is the mean magnetic moment $\bar{m}$ of the ensemble of nanoparticles. For this, we follow the Fokker-Planck (FP) equation approach for the Landau-Lifshitz-Gilbert equation as already described in [4]. From the general case as described in e.g. [7], we arrive at the form below. For a detailed discussion of the equation in the MPI context, see [3]. We determine $\bar{m}$ via the probability density function $f : \Omega \times \mathbb{S}^2 \times [0,T] \to \mathbb{R}_0^+$ which is the solution to the corresponding FP equation where $\mathbb{S}^2$ is the surface of the sphere in $\mathbb{R}^3$. The mean is then given by

$$\bar{m}_{\text{FP-anis}}(r,t) = m_0 \int_{\mathbb{S}^2} m f(r,m,t)\,\mathrm{d}m \tag{2}$$

where f is the solution to the following specific case of a convection-diffusion equation on the sphere

$$\frac{\partial}{\partial t} f = \text{div}_{\mathbb{S}^2}\left(\frac{1}{2\tau}\nabla_{\mathbb{S}^2} f\right) - \text{div}_{\mathbb{S}^2}\left(b f\right) \tag{3}$$

where $\tau > 0$ is the relaxation time constant and the (velocity) field $b : \mathbb{S}^2 \times \mathbb{R}^3 \times \mathbb{S}^2 \to \mathbb{R}^3$ given by

$$\begin{aligned} b(m,H,n) &= p_1 H \times m + p_2 (m \times H) \times m \\ &\quad + p_3 (n \cdot m) n \times m + p_4 (n \cdot m)(m \times n) \times m \end{aligned} \tag{4}$$

where $p_i \geq 0$, $i = 1,\ldots,4$, are physical constants and $n \in \mathbb{S}^2$ is the easy axis of the particles.

A Néel rotation including uniaxial anisotropy is then given by $p_1 = \tilde{\gamma}\mu_0$, $p_2 = \tilde{\gamma}\alpha\mu_0$, $p_3 = 2\tilde{\gamma}\frac{K^{\text{anis}}}{M_S}$, and $p_4 = \alpha p_3$ with $\tau = \frac{V_C M_S}{2k_B T_B \tilde{\gamma}\alpha}$ and $\tilde{\gamma} = \frac{\gamma}{1+\alpha^2}$. Here, V_C is the core volume of the nanoparticles depending on the core diameter D, and we have saturation magnetization M_S, damping parameter α, Boltzman constant k_B and temperature T_B, respectively. The uniaxial anisotropy constant is denoted by K^{anis}. We note that the parabolic partial differential equation in (3) has no dependence on derivatives with respect to the spatial variable r. It can thus be considered as parametric with respect to r, respectively the constant offset fields encoded in the selection field. The equation is solved numerically by using a finite volume method exploiting the computational toolbox provided in [8].

II.II. Equilibrium model with anisotropy

Over-simplified models like the standard *equilibrium model* (see, e.g., [3]) do not take into account the particles' anisotropy. But there exist equilibrium models that do consider anisotropy [5], which we exploit as follows: The probability function $g : \Omega \times \mathbb{S}^2 \times [0,T] \to \mathbb{R}_0^+$ is given by the Boltzmann distribution

$$g(r,m,t) = \frac{1}{Z(r,t)} e^{\beta(\mu_0 V_C M_S m \cdot H(r,t) + K^{\text{anis}} V_C (m \cdot n)^2)} \tag{5}$$

explicitly taking into account the Zeeman and the anisotropy energy for given easy axis $n \in \mathbb{S}^2$ ($\beta = \frac{1}{k_B T_B}$). Here, $Z(r,t) = \int_{\mathbb{S}^2} e^{\beta(\mu_0 V_C M_S m \cdot H(r,t) + K^{\text{anis}} V_C (m \cdot n)^2)} \, \mathrm{d}m$ is a normalization factor such that g is a probability density function with respect to m. The mean is then directly computed by evaluating the following integral

$$\bar{m}_{\text{EQA}}(r,t) = m_0 \int_{\mathbb{S}^2} m g(r,m,t) \, \mathrm{d}m. \tag{6}$$

Exploiting spherical coordinates, four 2D integrals have to be solved computationally for any tuple (r,t).

In order to compare the two models, we simulated an MPI system matrix for an 11×11 pixel 2D grid with a Lissajous trajectory for both cases. The simulations were carried out for different fixed easy axis orientations and different values for K^{anis} and D. Particle and scanner parameters are chosen according to [2].

III. Results

For comparing the simulation results, we chose the following error metric whose results are illustrated in Table 1: for each pixel, the ratio between the mean absolute error of $\partial_t \bar{m} = \frac{\partial}{\partial t} \bar{m}$ and its maximum amplitude in the Néel case is computed in the time domain. Then, the maximum of these errors is taken over all pixels $r \in \hat{\Omega} \subset \Omega$ and easy axis orientations $\theta \in \hat{\Theta}$:

$$\text{err} = \max_{\theta \in \hat{\Theta}, r \in \hat{\Omega}} \frac{T^{-1} \int_0^T |\partial_t (\bar{m}^{\theta}_{\text{FP-anis}}(r,t) - \bar{m}^{\theta}_{\text{EQA}}(r,t))|_1 \, dt}{\|\partial_t \bar{m}^{\theta}_{\text{FP-anis}}(r,\cdot)\|_\infty}.$$

Table 1: Errors of (EQA) relative to the Néel model for different core diameters and anisotropy constants, and blocking diameters D_{bl} for each K^{Anis}.

K^{Anis}[J/m^3]/D[nm]	16	20	24	D_{bl}[nm]
1100	5e-4	7e-4	1e-3	47
2100	5e-4	1e-3	3e-3	38
3100	6e-4	2e-3	9e-3	34
4100	7e-4	3e-3	2.5e-2	31
5100	9e-4	6e-3	5.4e-2	28
6100	1e-3	1.2e-2	0.15	26
7100	2e-3	2.5e-2	0.43	25

For smaller core diameters and anisotropy constants, the results from (EQA) differ only very slightly from the full Néel solution. However, for large values of D and K^{Anis}, the anisotropy energy barrier is larger than the thermal or applied magnetic energy and the particles enter a (partially) "blocked" state, exhibiting hysteresis and losing their superparamagnetic properties [9], which leads to large errors made by the EQA model. The critical blocking diameter D_{bl} can be calculated for given K^{Anis}, temperature and excitation frequency and is shown in Table 1.

An example for intermediate parameter values is displayed in Fig. 1. Here, two frequency components for the FP as well as the EQA case are shown for two different easy axis directions. The frequency k is expressed in terms of the mixing orders $k(\kappa_x, \kappa_y) = \kappa_x N_{\text{dens}} + \kappa_y (N_{\text{dens}} + 1)$, where N_{dens} is the parameter controlling the density of the Lissajous pattern. While the results are similar, a slight phase shift can be seen between the two simulations, especially for the larger one of the two frequencies. As Table 1 suggests, these phase shifts are nearly nonexistent for small parameters and become very significant for large ones.

IV. Discussion and conclusion

This work builds the initial step to explore the possibilities to use an equilibrium model-based approach in the dedicated application of immobilized nanoparticles in MPI. The results indicate that this can be done for a certain range of particle parameters keeping the relative error below 1% when compared to the FP Neél model. This fosters the way for immediate future research on a validation on measured data and the development of coupled models taking into account the presented equilibrium model with uniaxial anisotropy.

Acknowledgments

The authors would like to thank T. Knopp and his group for many fruitful discussions as well as the anonymous reviewer of [2] for pointing out [5], which inspired this work. H. Albers and T. Kluth acknowledge funding by the German Research Foundation (DFG) - project 426078691.

Author's statement

Authors state no conflict of interest.

References

[1] M. Möddel, F. Griese, T. Kluth, and T. Knopp. Spatial orientation estimation of immobilized magnetic nanoparticles with parallel aligned easy axes. *Physical Review Applied*, 2021, In print.

[2] H. Albers, T. Knopp, M. Möddel, M. Boberg, and T. Kluth. Modeling the magnetization dynamics for large ensembles of immobilized magnetic nanoparticles in multi-dimensional magnetic particle imaging. *Journal of Magnetism and Magnetic Materials*, 543:168534, 2022, doi:https://doi.org/10.1016/j.jmmm.2021.168534.

[3] T. Kluth. Mathematical models for magnetic particle imaging. *Inverse Problems*, 34(8):083001, 2018.

[4] T. Kluth, P. Szwargulski, and T. Knopp. Towards accurate modeling of the multidimensional magnetic particle imaging physics. *New Journal of Physics*, 21(10):103032, 2019, doi:10.1088/1367-2630/ab4938.

[5] M. Hanson, C. Johansson, and S. Morup. The influence of magnetic anisotropy on the magnetization of small ferromagnetic particles. *Journal of Physics: Condensed Matter*, 5(6):725–732, 1993, doi:10.1088/0953-8984/5/6/009.

[6] Mark, Mat2rgbcmplx, MATLAB Central File Exchange, 2021. URL: https://www.mathworks.com/matlabcentral/fileexchange/52876-mat2rgbcmplx.

[7] W. T. Coffey, P. J. Cregg, and Y. U. P. Kalmykov, On the theory of debye and néel relaxation of single domain ferromagnetic particles, in *Advances in Chemical Physics*. John Wiley & Sons, Inc., 1992, 263–464, ISBN: 9780470141410. doi:10.1002/9780470141410.ch5.

[8] H. Albers, T. Kluth, and T. Knopp. Simulating magnetization dynamics of large ensembles of single domain nanoparticles: Numerical study of Brown/Néel dynamics and parameter identification problems in magnetic particle imaging. *Journal of Magnetism and Magnetic Materials*, 541:168508, 2022, doi:https://doi.org/10.1016/j.jmmm.2021.168508.

[9] C. Binns, Chapter 1 - tutorial section on nanomagnetism, in *Nanomagnetism: Fundamentals and Applications*, ser. Frontiers of Nanoscience, C. Binns, Ed., 6, Elsevier, 2014, 1–32. doi:https://doi.org/10.1016/B978-0-08-098353-0.00001-4.

